Ultrathin magnetic films: Electrochemistry versus molecular-beam epitaxy

W. Schindler and J. Kirschner
Max-Planck-Institut für Mikrostrukturphysik, Weinberg 2, 06120 Halle, Germany
(Received 26 August 1996)

Ultrathin Co films have been electrodeposited on Cu(001) from an aqueous $Na_2SO_4/CoSO_4$ electrolyte under cleanliness conditions equivalent to ultrahigh vacuum of 5×10^{-10} mbar. Films thicker than 1.5 ML show in-plane magnetization and square hysteresis loops. The saturation magnetization increases linearly with film thickness. The magnetization vanishes below 1.5 ML in agreement with molecular-beam epitaxy (MBE) films at 300 K. The coercivity varies approximately linearly with film thickness and is ten times larger than usually observed in MBE-grown Co. ''Magnetically dead'' layers have not been found.
[S0163-1829(97)52104-7]

About 25 years ago the field of thin film magnetism experienced an intensive renaissance as a consequence of reports by Liebermann *et al.* on ''magnetically dead'' layers at the surface of very thin Fe, Ni, and Co films.[1,2] This spurred a great deal of theoretical and experimental effort to investigate the magnetic properties of dimensionally reduced systems. However, over the years it became clear that the initial observations had to be attributed to contaminated surfaces and interfaces. Since the ''dead layer'' films had been prepared by electrodeposition, the general belief evolved that this method was not suitable to produce clean epitaxial magnetic films in the monolayer range.

In this paper we show that this prejudice is wrong. We do this by choosing the system Co on Cu(001), which has been very well characterized in numerous molecular-beam epitaxy (MBE) experiments in ultrahigh vacuum (UHV) and which is known to grow epitaxially and layer by layer due to the small difference in the lattice constants of $<2\%$.[3–6] We compare the magnetic characteristics of our electrochemically deposited films, as measured in the electrochemical cell, to those of films prepared by MBE in UHV. We find very good agreement, with the exception of the coercive fields, and clearly demonstrate the absence of ''magnetically dead'' layers under carefully controlled experimental conditions. We show that the contamination level in the electrolytical cell can be reduced to that of UHV conditions, even for a relatively reactive material such as cobalt. We conclude that there should be no principal obstacles to fully exploit the technologically very attractive features of electrodeposition: large area deposition, low material consumption, suitability for mass production, fast processing, and low cost of equipment.

Co has been deposited in the ML range on Cu(001) crystals from an aqueous electrolyte of 0.3 M Na_2SO_4 and 1 mM $CoSO_4$ in an electrochemical cell (Fig. 1), which allows the *in situ* measurement of the magnetization by the magneto-optical Kerr effect[7] (MOKE) using a HeNe-laser beam. The cell is similar to that described in Ref. 8.

The Cu crystals were oriented and mechanically polished to better than 0.2° deviation as measured by x-ray diffraction. All areas of the Cu crystals except the oriented surface have been isolated with a commercial lacquer to prevent contact of other crystallographic orientations to the electrolyte. The Cu surface was electrochemically polished in 65% H_3PO_4 at potentials of $+1.8\cdots+2.4$ V against a carbon electrode for several minutes. Then the substrates were transferred into the electrochemical cell under the protection of ultrapure water (Milli Q plus). Immediate connection to the potentiostat at -200 mV versus the standard calomel reference electrode (SCE) provided cathodic protection of the Cu surface. The pH value of the electrolyte was 4.5–5 and dissolved oxygen was removed from the electrolyte by degassing with ultrapure N_2.

The deposition of the Co films has been controlled by the current-voltage characteristics as shown in Fig. 2. The deposition and subsequent dissolution of the films is a reversible process, which can be repeated many times simply by cycling the potential of the substrate as indicated by the arrows in Fig. 2. The Co deposition has been done at a potential of -800 mV. The film thickness is calculated from the mea-

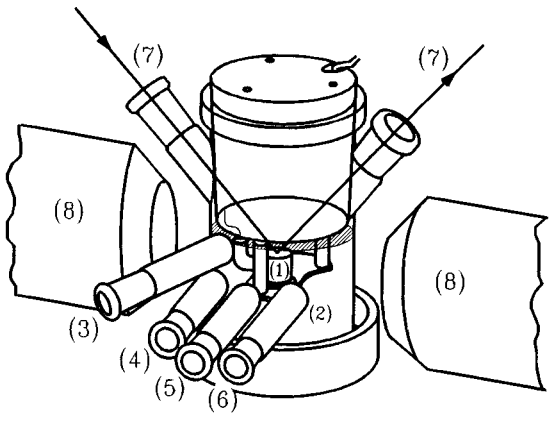

FIG. 1. Electrochemical cell for the electrodeposition of ultrathin films with simultaneous MOKE measurements in a magnetic field: The potential is applied in a standard electrochemical configuration at the Cu crystal (1) against a remote electrode [(5), Pt wire] with respect to the reference electrode [(3), standard calomel electrode] in an aqueous electrolyte (2); The magnetic field (8) is applied in the [110] direction and in the plane of the laser beam (7) for the longitudinal MOKE measurements. Additional measurement facilities can be inserted into other joints of the cell (4, 6).

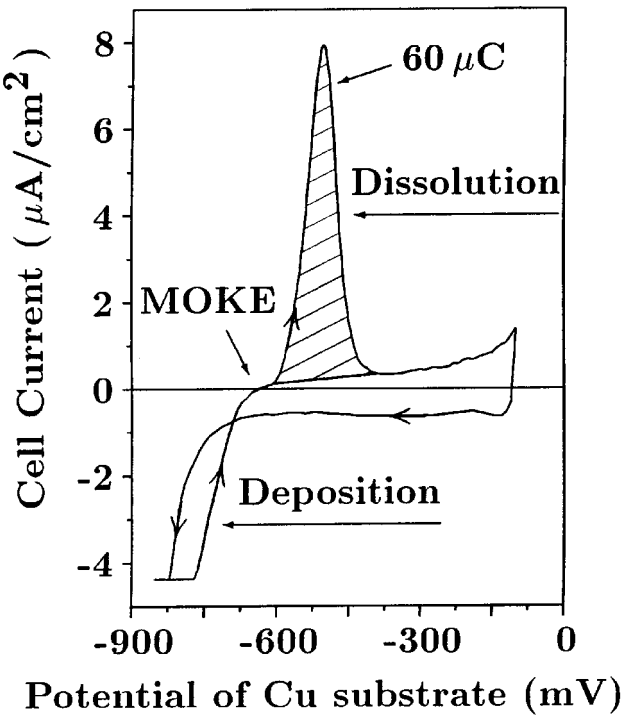

FIG. 2. Current-voltage characteristics of the Co deposition from an aqueous 0.3 M Na_2SO_4 and 1 mM $CoSO_4$ electrolyte. The arrows indicate the cycling direction (with 10 mV/s) of the reversible deposition/dissolution process. The Co films are deposited at potentials below -750 mV. The anodic peak around -500 mV (dashed area) represents the dissolution of the previously deposited Co film and corresponds to a charge of 60 μC or a film thickness of 0.15 ML. The MOKE measurements are done at that specific potential where no external current flows to or from the substrate.

sured charge (i.e., integral of the anodic peak, dashed area in Fig. 2) during the dissolution of the Co film at a potential around -500 mV, the geometrical area of the Cu substrates and the bulk-Co lattice constant of 0.351 nm. A thickness resolution of 0.02 ML can be achieved from the current-voltage characteristics. This is practically reduced by possible incomplete dissolution of the first Co monolayer seen as enhanced anodic current at potentials between -400 mV and -100 mV or by variation in the base current. The reproducibility as proven by the independent thickness measurement by MOKE is better than 0.2 ML. The stability of the films during the MOKE measurements has been achieved by adjusting the potential of the Cu substrate to that specific value between the deposition and dissolution potential of the Co films as indicated in Fig. 2, where nearly no external current flows to or from the substrate.

The purity conditions of the electrolytic environment are determined by two major factors: Contamination by organic reagents and ions.

The organic contaminations result mainly from the Milli Q water purification system and are less than 50 ppb corresponding to less than 10^{17} organic particles in our cell volume of 100 ml. The specific resistance of the ultrapure water is larger than 18.2 MΩ cm. This results nominally in a current density of approximately 50 nA/cm^2 or equivalently in an exposure of a 1 cm^2 substrate of 10^{-4} ML/s assuming single charged ions. Ionic contaminations of ultrapure Na_2SO_4 and $CoSO_4$ electrolyte salts are less than 2×10^{-5} (Aldrich and Merck suprapure grade). Our typical concentration of the electrolyte salts of 0.3 M Na_2SO_4 and 1 mM $CoSO_4$ and typical mobilities of ions in water of approximately 10^{-3} cm^2 V^{-1} s^{-1} (Ref. 9) lead to an exposure of the substrate of 10^{-3} ML/s.

The measured current density in the cell as derived from the current-voltage characteristics (Fig. 2) is approximately 0.6μA/cm^2 for cell potentials between -700 mV and -100 mV. This gives a maximum experimental estimate for the nominal exposure of the substrate of 10^{-3} ML/s. This would then correspond to a deposition of approximately 1 ML of unwanted material in 1000 s assuming a sticking probability of 100%. We may compare this directly to UHV conditions: At 5×10^{-9} mbar a monolayer of contamination forms on Cu(001) in 1000 s, again assuming unity sticking probability.

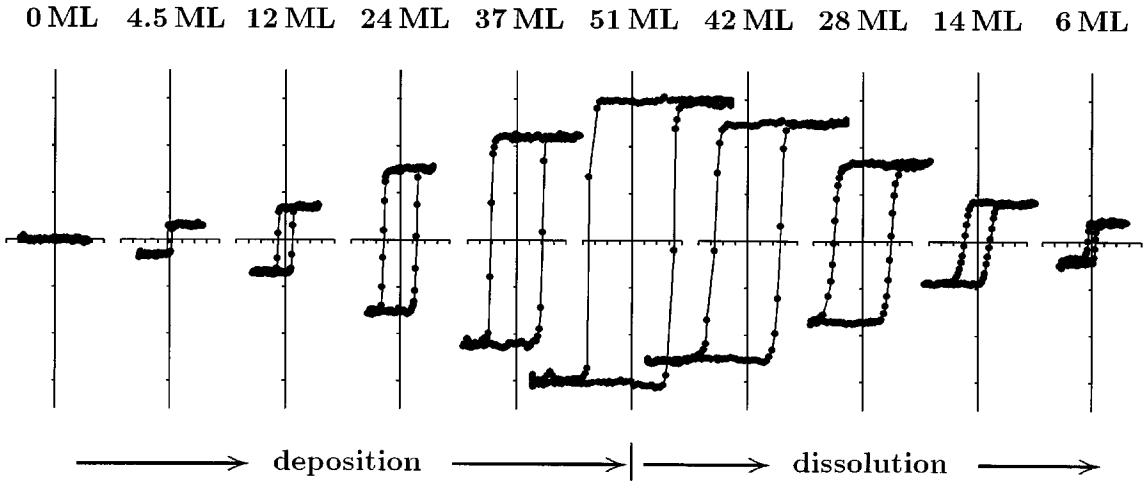

FIG. 3. Thickness dependence of the in-plane magnetization and the coercive field at room temperature (298 K). The sequence of measurements has been taken during the deposition of a single film and its subsequent dissolution. The deposition potential was -890 mV, the MOKE measurements have been performed at -670 mV. The x axis is ±30 mT for all graphs. The y axis is the same for all graphs (a.u.). The measurement time of each complete magnetization cycle was approximately 20 s.

However, this rough estimate of the maximum exposure does not consider the peculiarities of electrochemistry: First, base metal contaminations as, for example, Fe, Cd, Mg, Ca, Al, and rare earth or alkali metals are remaining in the electrolyte without deposition onto the substrate according to the electrochemical standard potentials. Second, base metal contaminations with Nernst potentials in the negative potential range between -700 mV and -100 mV as Ni, Mo, Sn, or Pb could be experimentally seen as a deposition/dissolution peak with a charge resolution of 0.02 ML in the current-voltage characteristics if present. Third, anionic contaminations as for example the SO_4^{2-} or Cl^- anions lead to an absorption at the substrate surface or adlayer formation, which in fact determines the microscopic growth of the metal films.[10] Those adlayer atoms need not necessarily be incorporated into the metal films as contaminations. And finally, the cell current in the negative potential range around -300 mV does not exclusively result from ions but also from oxygen reactions.[11] From the low base current of less than 0.6 $\mu A/cm^2$ in Fig. 2 it can be seen that these reactions can be eliminated by careful *in situ* saturation of the electrolyte with N_2 gas.

These electrochemical considerations reduce the maximum possible ionic contamination level of the films further from 10^{-3} ML/s as estimated above to less than 10^{-4} ML/s, which is equivalent to UHV conditions of 5×10^{-10} mbar. This shows that electrochemical deposition techniques can be as ''clean'' as molecular-beam epitaxy in ultrahigh vacuum.

The magnetic properties of ultrathin films respond sensitively to contamination, in particular, in the monolayer range. Therefore we combined our electrochemical cell with *in situ* magneto-optical Kerr effect measurements at ambient temperature (298 K). The magnetic field was oriented along the easy [110] direction.

The sequence of magnetization curves in Fig. 3 is taken during the growth and dissolution of a single Co film. The electrodeposition technique uniquely allows measurements not only during deposition but also during the dissolution of films. The magnetic hysteresis as derived from the 1-mm^2 unfocused laser spot on the surface is rectangular shaped up to the thickest films of 51 ML (Fig. 3) showing that the films are of even thickness across the measured surface area. The easy axis of the magnetization is in plane as is known from MBE-grown films.[3,4,6] The remanence at zero external field equals the saturation magnetization due to the nearly square hysteresis loops.

The saturation magnetization of the films depends linearly on the Co thickness above a thickness of 2 ML [Figs. 4(a) and 4(b)]. The vanishing magnetization below 1.5 ML in our measurements is ascribed to the decrease of the Curie temperature with decreasing film thickness and the lack of percolation of Co islands at coverages below 1 ML. This magnetic behavior is exactly observed in MBE-grown Co/Cu(001) films.[3–5] The linear fit in Fig. 4(a) extrapolates to zero magnetization for 0 ML within the experimental accuracy [Fig. 4(b)]. This allows the conclusion that each Co monolayer contributes to the total magnetization of the film. This clearly shows that there are no ''magnetically dead'' layers in our electrodeposited Co films. The onset of the magnetization at 1.5 ML and the square magnetic hysteresis

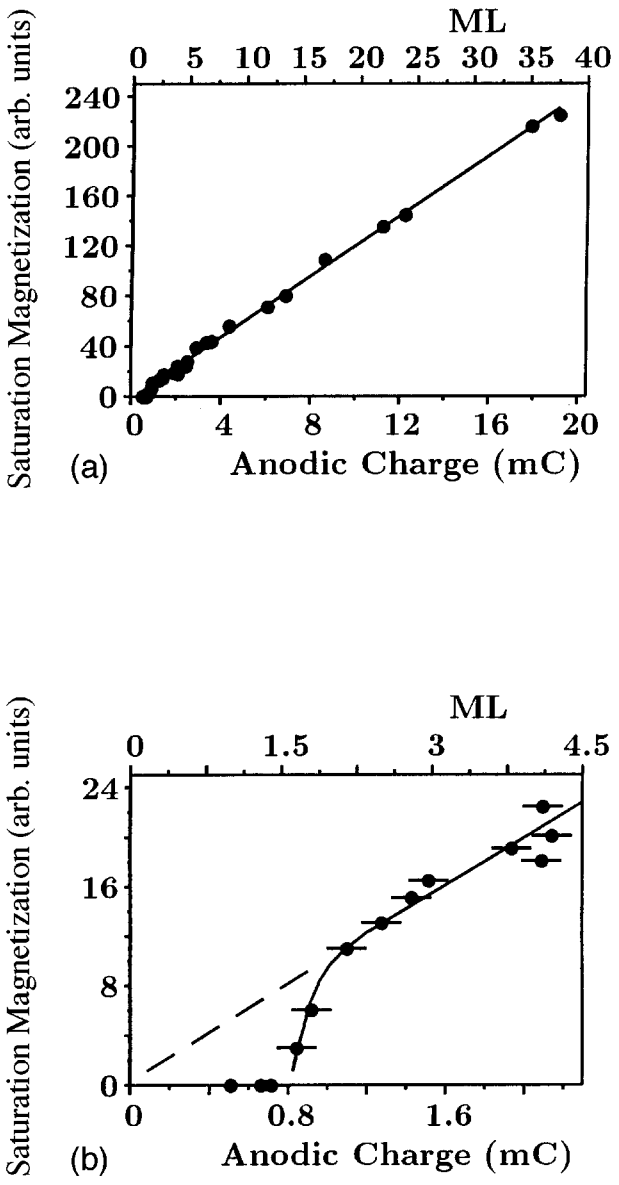

FIG. 4. (a) Dependence of the total saturation magnetization on the number of ML (upper x scaling) corresponding to the deposited charge (lower x scaling). The magnetic field is applied in the easy [110] direction. The linear fit through the data points above 2 ML extrapolates to zero for 0 ML film thickness. (b) Total saturation magnetization of films up to a thickness of 4.5 ML (upper x scaling). The corresponding deposited charge is shown in the lower x scaling. The error bars indicate ±0.2 ML. The linear fit through the data points above 2 ML as seen in Fig. 4(a) extrapolates to zero for 0 ML film thickness (dashed line).

are compatible with a layer-by-layer growth mode in the initial stages of the deposition as is known from MBE-deposited Co films.

The coercive field H_C of the films varies approximately linearly with the film thickness, starting from 0.9 mT at 2.5 ML and ranging to 25 mT at 51 ML (Fig. 3). H_C is approximately ten times larger than it is usually observed in MBE-grown Co films of the same thickness (see, for example, Refs. 4 and 5). Remarkably, H_C is not enhanced by protective cover layers, because all measurements have been done *in situ* at the free Co surface. Since the magnetic field

has been adjusted along the easy [110] direction, the measured H_C is the minimum due to the in-plane magnetization anisotropy of Co(001), which shows the hard axis in the [100] direction.[3] This large coercivity could be attributed to the electrodeposition technique, which may produce a certain defect structure of the Co films favorable for domain wall pinning. The known double-layer growth of MBE films could be different in electrodeposited films due to the deposition near the thermodynamical equilibrium in the electrochemical environment. This argument is supported by recent scanning tunneling microscopy observations, which show that different preparation methods result in different film growth behavior and accordingly in different magnetic properties, like MBE growth and pulsed laser ablation of ultrathin Fe films on Cu(111) (Ref. 12) or ion beam sputtering and dc sputtering of Co/Cu multilayers.[13] Also the substrate preparation by our electrochemical polishing, compared to the usual sputtering/heating procedure during an UHV preparation of crystals (see, for example, Ref. 14), is likely to cause additional domain wall pinning in our electrodeposited films compared to evaporated films.

The electrodeposition of ultrathin magnetic films has been shown to be capable of depositing magnetic films in the monolayer range under conditions similar to UHV conditions and with similar properties as are known from MBE-deposited films. We clearly demonstrated that there are no ''magnetically dead'' layers in our electrodeposited films. In particular, the reproducible preparation of ultrathin clean films in the monolayer range with a fast and cost effective technique like the electrodeposition opens interesting prospects. A unique feature of the electrochemistry is the possibility to finely adjust the film thickness by deposition and dissolution. This may even be done *in situ* controlled by a magnetic measurement such as MOKE. Thus, films or sequences of layers with exactly the desired magnetic properties may be obtained by using appropriate feedback circuits. This might be of significant technological relevance for potential applications of electrodeposited films.

We are indebted to H. Menge for the preparation of the Cu crystals.

[1] L. N. Liebermann, D. R. Fredkin, and H. B. Shore, Phys. Rev. Lett. **22**, 539 (1969).

[2] L. N. Lieberman, J. Clinton, D. M. Edwards, and J. Mathon, Phys. Rev. Lett. **25**, 232 (1970).

[3] P. Krams, F. Lauks, R. L. Stamps, B. Hillebrands, and G. Güntherodt, Phys. Rev. Lett. **69**, 3674 (1992).

[4] H. A. Wierenga, W. de Jong, M. W. J. Prins, Th. Rasing, R. Vollmer, A. Kirilyuk, H. Schwabe, and J. Kirschner, Phys. Rev. Lett. **74**, 1462 (1995).

[5] T. Suzuki, D. Weller, C.-A. Chang, R. Savoy, T. Huang, B.A. Gurney, and V. Speriosu, Appl. Phys. Lett. **64**, 2736 (1994).

[6] J. R. Cerda, P. L. de Andres, A. Cebollada, R. Miranda, E. Navas, P. Schuster, C. M. Schneider, and J. Kirschner, J. Phys. Condens. Matter **5**, 2055 (1993).

[7] S. D. Bader, J. Magn. Magn. Mater. **100**, 440 (1991).

[8] W. Schindler and J. Kirschner Rev. Sci. Instrum. **67**, 3578 (1996).

[9] R. A. Robinson and R. J. P. Williams, *Electrolyte Solutions* (Butterworth, London, 1959).

[10] O. M. Magnussen, J. Hotlos, R. J. Nichols, D. M. Kolb, and R. J. Behm, Phys. Rev. Lett. **64**, 2929 (1990).

[11] J. P. Hoare, in *Standard Potentials in Aqueous Solution*, edited by A. J. Bard, R. Parsons, and J. Jordan (Marcel Dekker, New York, 1985), p. 49.

[12] H. Jenniches, M. Klaua, H. Höche, and J. Kirschner, Appl. Phys. Lett. **69,** 3339 (1996).

[13] T. J. Minvielle, R. J. Wilson, and R. L. White, Appl. Phys. Lett. **68**, 2750 (1996).

[14] J. Shen, J. Giergiel, A. K. Schmid, and J. Kirschner, Surf. Sci. **328**, 32 (1995).